

Supporting Information :

Calibration and application of large-scale LIBS project based on transfer learning in online quantitative analysis of coal

AN LI, XINYU ZHANG, XIAODONG LIU, HAOHAN SUN, and RUIBIN LIU*

Key Lab of Precision Spectroscopy and Optoelectronic Technology, School of Physics, Beijing Institute of Technology, Beijing 100081, China.

*liusir@bit.edu.cn

1. The off-line LIBS system

The offline bench-top LIBS detection equipment is calibrated using standard coal samples. Upon verification of prediction accuracy using blind samples, which satisfies the requirements of national standards, the offline bench-top LIBS equipment can serve as a rapid standard measurement device for the online analysis of material composition. This device can replace the laboratory assays that typically take several hours and act as an auxiliary system for the quick verification of calibration and prediction effects of online LIBS equipment.

The off-line LIBS system used in this work is an integrated industrial apparatus (BrightRay Laser Technology Ltd, Suzhou, China), as shown in Fig.S1. The laser beam with a diameter of 4 mm and energy of 100 mJ output from a Q-switched Nd: YAG laser (Ultra 100, 1064 nm, Quantel, USA), and the laser pulse duration is around 7 ns. The laser irradiates on the sample surface by a quartz lens L_1 (focus length $f=100$ mm) with a repeat frequency of 5 Hz. An x - y - z 3D electrical motor drives the sample stage T with a motion step of 10 μm . The step program controls the sample stage moving forward 1 mm every five laser pluses and yields an ablation point grid with 7×6 points on the sample surface. The signal acquisition part consists of an optical fiber of 200 μm in diameter installed in the fiber holder and a quartz lens L_2 with a numerical aperture (NA) of 0.25 and a focal length of 10 mm. The spectra are acquired for one sample by a four-channel spectrometer (Avantes Avsdesktop USB3.0, Netherlands) with a resolution of 0.1 nm. A charge-coupled device (CCD) with 2048 pixels on each channel is installed. The gate of the spectrometer is controlled by a Q switch signal of the laser pulse as an external trigger source.



Fig.S1. The off-line LIBS machine, R1: mirror, L1/L2: lens, S: sample stage

2. The calibration of source online LIBS system.

- (1) 300 spectra are collected online at a sampling frequency of 1 Hz, while the material on the conveyor belt is sampled through the factory-installed crushing, dividing, and sampling device, extracting 500 g of coal material. The sampling device ensures that during the spectrum collection period, the coal material is uniformly sampled.
- (2) The extracted 500g of bulk material is dried and then ground into a powder with a particle size of <200 μm . An appropriate amount of this powder is taken and pressed into a coal pellet with a diameter of 30 mm and a thickness of 4 mm using a 20-ton press.
- (3) Steps (1) and (2) are repeated enough times to obtain over 30 coal cakes in total. These cake-shaped coal samples are then analyzed using the offline LIBS equipment to acquire the reference values for the total moisture content, ash, sulfur, and calorific value of the samples. A quantitative analysis model is established using the spectral data collected by the online device and the corresponding reference values of the various parameters in the coal. This model is referred to as the source model (Model-1). Before model training, the spectral data of each sample are preprocessed in following several steps. Firstly, obtain the effective coal spectra by the feature comparison method mentioned in the main text according to step (1)~(4), and then the spectra must be standardized, which means that more stable data should be selected based on the statistical criteria, as described in our previous work^{1,2}. Based on the Eq. (1) ~ Eq. (3).

$$S_X^T = \begin{bmatrix} I_{11} & I_{11} & I_{11} & \cdots & I_{1j} \\ I_{21} & I_{22} & I_{23} & \cdots & I_{2j} \\ I_{31} & I_{32} & I_{33} & \cdots & I_{3j} \\ \vdots & \vdots & \vdots & \ddots & \vdots \\ I_{n1} & I_{n1} & I_{n1} & \cdots & I_{nj} \end{bmatrix} \quad (1)$$

$$M_{S_X} = \left[\begin{array}{cccc} \frac{\sum_{j=1}^j I_{1j}}{j} & \frac{\sum_{j=1}^j I_{2j}}{j} & \frac{\sum_{j=1}^j I_{3j}}{j} & \cdots & \frac{\sum_{j=1}^j I_{ij}}{j} \end{array} \right]^T \quad (2)$$

$$[M_{Sx} - \sigma, M_{Sx} + \sigma] \quad (3)$$

Where S_x^T indicates the spectrum of an ore sample, I_{nj} is the signal intensity of pixel j in n -th measurement, M_{Sx} is the mean value of the matrix S_x by row ($j = 10240$, n is defined by the coal spectra selection algorithm), the range of effective spectral data is defined by the average value M_{Sx} and the standard deviation σ of M_{Sx} .

- (4) Subsequently, the continuous background are removed based on the overlapped-window sliding (OWS) method, which is mentioned in our previous work³. This method allows for the overlap between various windows during the sliding processes, the width of window can be larger than the slide step, indicating more local minima are taken into account in background fitting while maintaining a wider width of the sliding window. After removing the continuous background, the shape of the peak does not deform or distort.
- (5) Finally, two-step spectral normalization method are performed³. Firstly, the continuous background of the spectrum in the subchannel is firstly utilized to normalize the spectral intensity, because the signal fluctuations with the continuous background are mainly induced by the bremsstrahlung radiation, which is correlated to the electronic temperature in the plasma⁴. It demonstrates that the spectral signal is normalized to a certain stable plasma state. The secondary normalization step uses the whole spectral strength in each subchannel to normalize the spectrum.
- (6) Each sample spectra are treated form (3) ~ (5), and the principal component analysis based partial least squares (PCA-PLS) model is established, and the hyperparameter is determined by the 5-fold cross-validation, the prediction results from establishing this model are shown in Fig.S2.

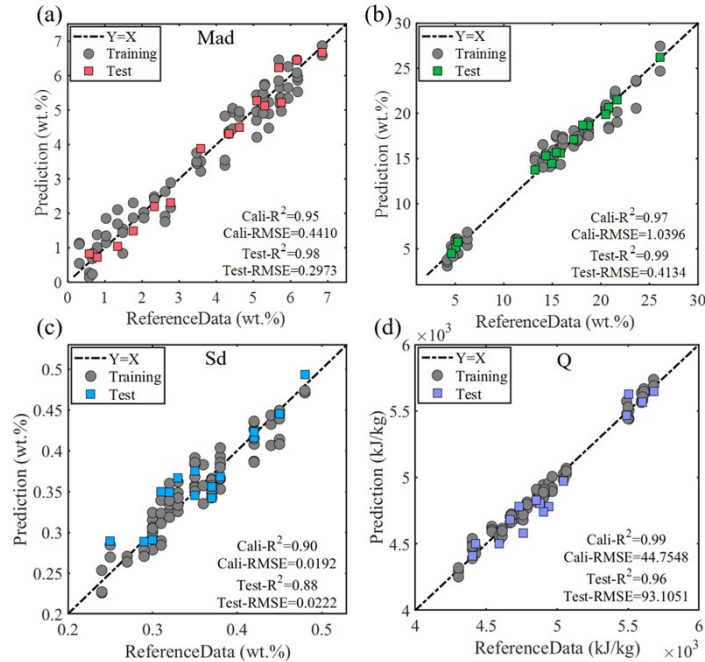


Fig.S2. Calibration results for online device 1: (a) Moisture content. (b) Ash content on a dry basis. (c) Total sulfur on a dry basis. (d) Calorific value.

3. The spectral similarity of transferred and source device.

As shown in Figure S3 (a), the comparison of the relative intensities of the spectra collected from the

same coal sample by the LIBS devices on production lines 1 and 2 shows that the number of characteristic peaks with an intensity variation of <10% accounts for about 91%. Fig.S3 (b) indicates that the number of peaks with a shift in the spectral features accounts for approximately 2.1% of the total number of peaks. Based on the spectral intensity similarity and the number of spectral feature peak shifts, the LIBS online devices on the two production lines meet the criteria for model transfer.

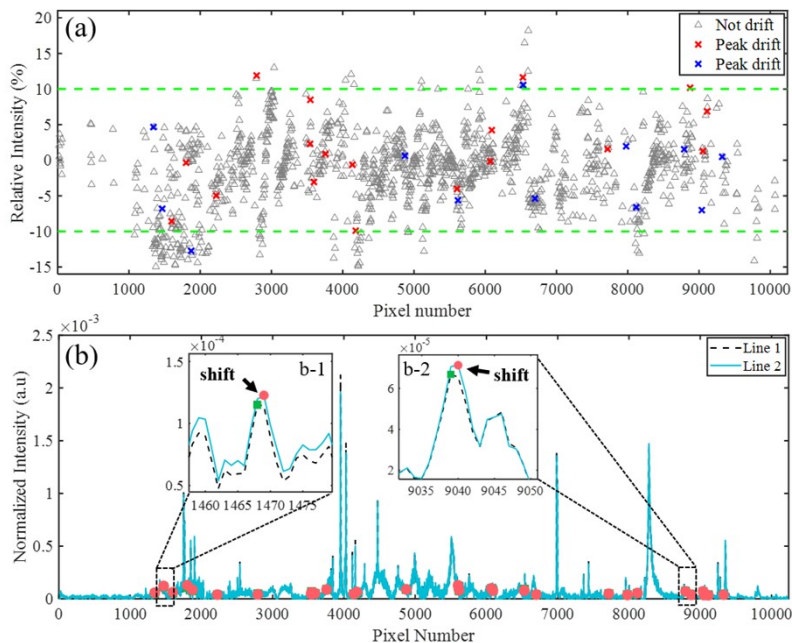


Fig. S3. Comparative spectral analysis of the same coal sample by LIBS equipment on production lines 1 and 2: (a) Comparison of relative spectral intensities; (b) Comparison of spectral peak shifts.

4. The online measurement results of line 1, line 3, and line 4.

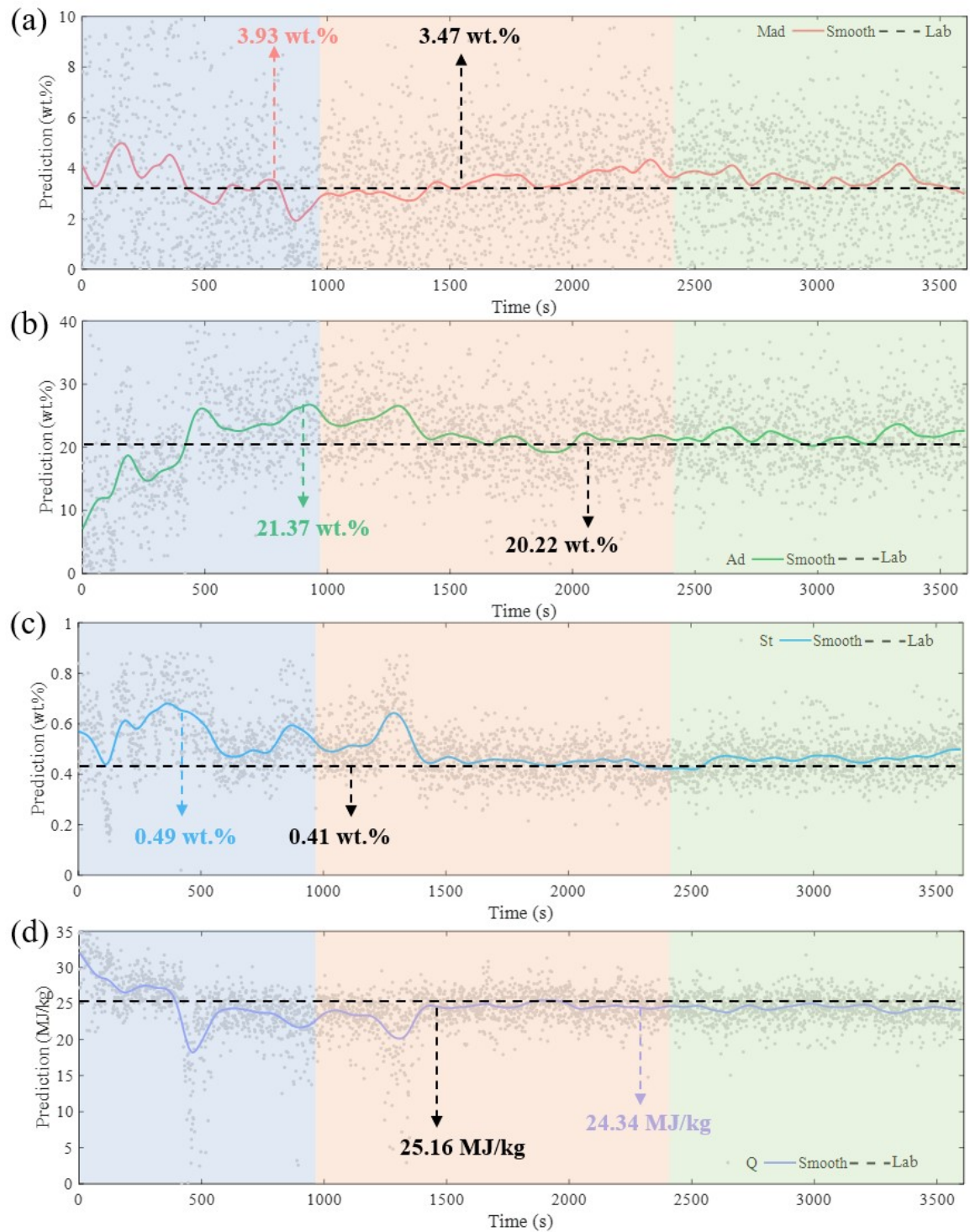


Fig.S4. Presents the online prediction results of system 1 on production line 1 using the source model for (a) moisture content. (b) dry basis ash content. (c) total sulfur content. (d) calorific value. The colored lines represent the average values within a 10-second interval, and the black dashed lines correspond to the assay values obtained from samples analyzed in the laboratory.

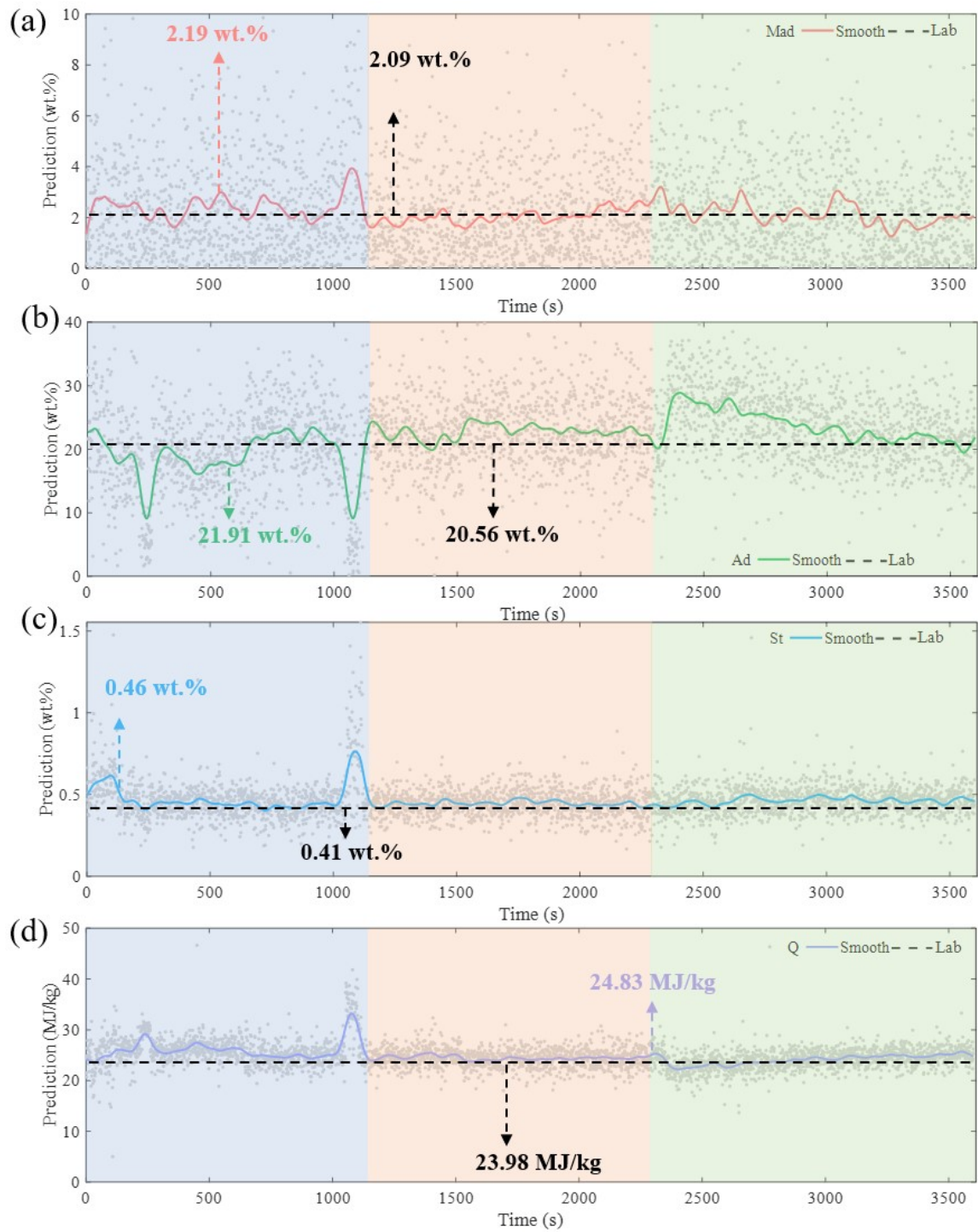


Fig.S5. Presents the online prediction results of system 3 on production line 3 using the transfer model for (a) moisture content. (b) dry basis ash content. (c) total sulfur content. (d) calorific value. The colored lines represent the average values within a 10-second interval, and the black dashed lines correspond to the assay values obtained from samples analyzed in the laboratory.

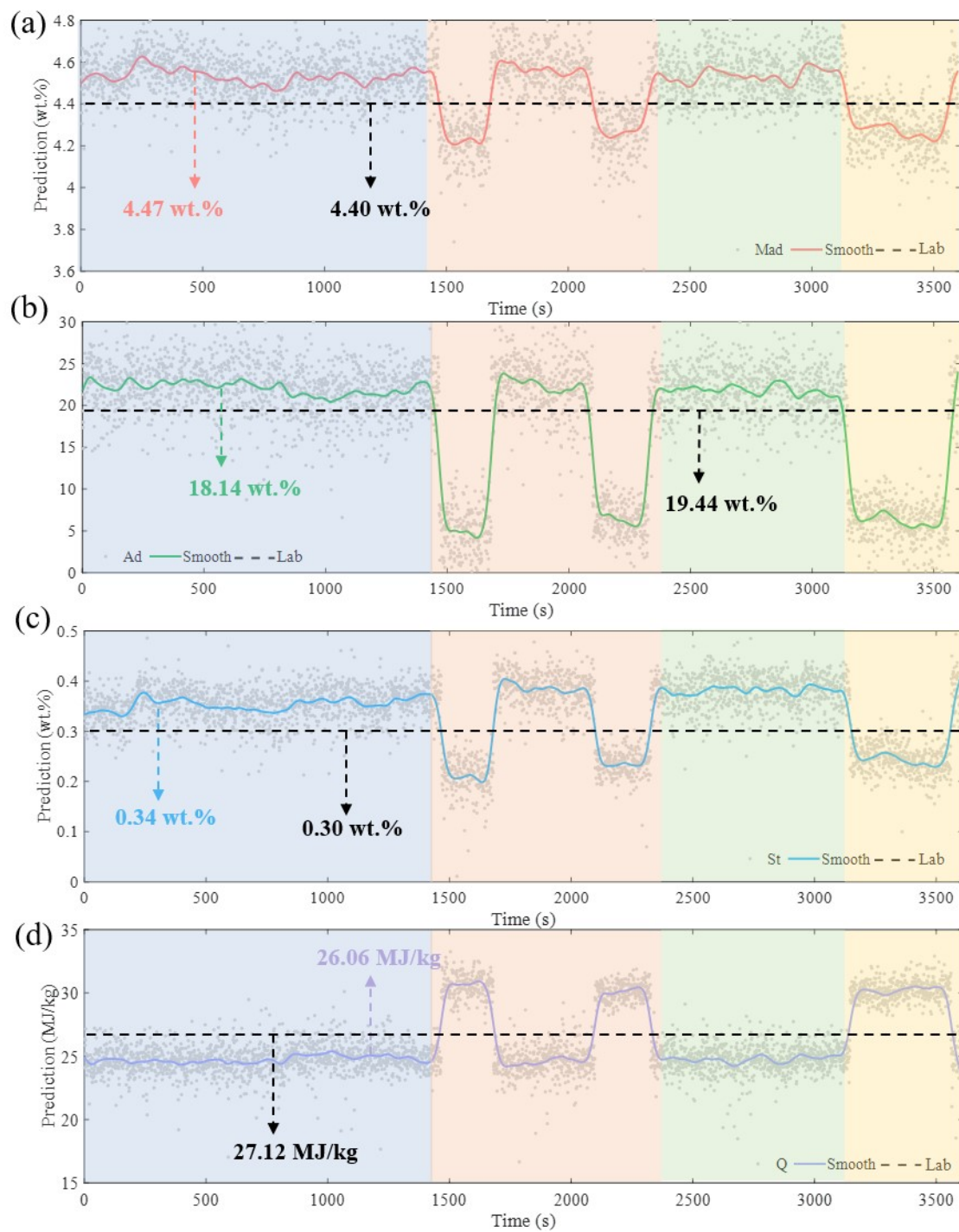


Fig.S6. Presents the online prediction results of system 4 on production line 4 using the transfer model for (a) moisture content. (b) dry basis ash content. (c) total sulfur content. (d) calorific value. The colored lines represent the average values within a 10-second interval, and the black dashed lines correspond to the assay values obtained from samples analyzed in the laboratory.

5. The comparison of applying source model to other production line directly.

Table.S1 Applying source model to system 2 on production line 2

Production line2	Moisture (wt.%)	Ash (wt.%)	Sulfur (%)	Calorific (MJ/kg)
Laboratory	3.51	19.61	0.38	24.03

<i>Applied source model to production line 2 directly</i>				
Prediction	6.38	30.22	1.04	11.57
MAE	2.87	10.61	0.66	12.46
<i>Applied transferred model to production line 2</i>				
Prediction	2.98	20.59	0.48	23.58
MAE	0.53	0.98	0.10	0.45

Table.S2 Applying source model to system 3 on production line 3

Production line3	Moisture (wt.%)	Ash (wt.%)	Sulfur (%)	Calorific (MJ/kg)
Laboratory	2.09	20.56	0.41	23.98
<i>Applied source model to production line 3 directly</i>				
Prediction	0.25	37.24	0.09	13.26
MAE	1.84	16.68	0.32	10.72
<i>Applied transferred model to production line 3</i>				
Prediction	2.19	21.91	0.46	24.83
MAE	0.10	1.35	0.05	0.85

Table.S3 Applying source model to system 4 on production line 4

Production line4	Moisture (wt.%)	Ash (wt.%)	Sulfur (%)	Calorific (MJ/kg)
Laboratory	4.40	19.44	0.30	27.12
<i>Applied source model to production line 4 directly</i>				
Prediction	1.12	8.66	0.01	40.37
MAE	3.28	10.78	0.29	13.25
<i>Applied transferred model to production line 4</i>				
Prediction	4.47	18.14	0.34	26.06
MAE	0.07	1.3	0.04	1.06

Reference

1. L. An, X. Zhang, X. Wang, Y. He, Y. Yin and R. Liu, *Journal of Analytical Atomic Spectrometry*, 2022, **37**, 2022-2032.
2. A. Li, X. Zhang, Y. Yin, X. Wang, Y. He, Y. Shan, Y. Zhang, X. Liu, L. Zhong and R. L. ab, *Journal of Analytical Atomic Spectrometry*, 2023, 810-817.
3. A. Li, X. Zhang, X. Liu, Y. He, Y. Shan, H. Sun, W. Yi and R. Liu, *Optics Express*, 2023, **31**,

38728-38743.

4. S. Zhang, X. Wang, M. He, Y. Jiang, B. Zhang, W. Hang and B. Huang, *Spectrochimica Acta Part B: Atomic Spectroscopy*, 2014, **97**, 13-33.